ACS OMEGA

Open Access

http://pubs.acs.org/journal/acsodf

Article

Hydrogeochemical Disparities and Constraints of Water Produced from Various Coal Seams in the Baode Block, Ordos Basin, China

Yuan Bao,* Yonghui Hao, Zhidong Guo, Yiliang Hu, Jiajun Li, Jiahao Meng, and Fei Wang

Cite This: *ACS Omega* 2024, 9, 4905−4919

Read Online

ACCESS | Metrics & More | Article Recommendations

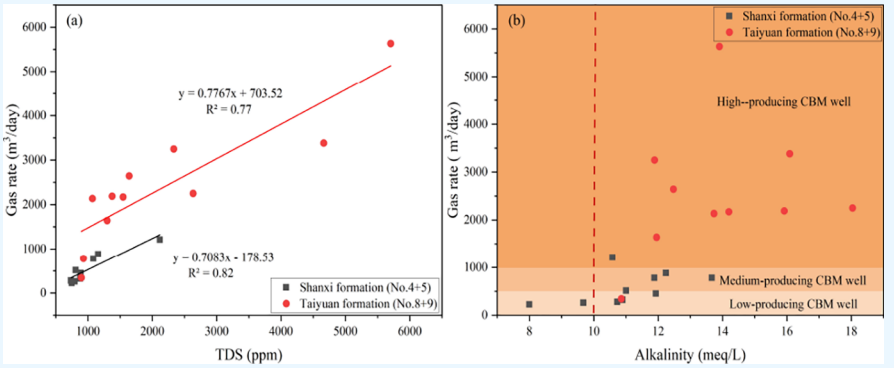

ABSTRACT: The hydrogeochemical characteristics of coalbed water play a crucial role in assessing the production level of coalbed methane (CBM) due to its involvement in the entire process of CBM generation, migration, accumulation, and extraction. To investigate variations in hydrochemical characteristics and controlling factors among different coal seams, a representative CBM field (Baode block) within the Ordos basin in China was chosen as a target. We have systematically collected produced water samples from coal seams of the Permian Shanxi Formation (P_1s) and Taiyuan Formation (P_1t). Tests and analyses were conducted on conventional cation and anions, trace elements, pH value, total dissolved solids (TDS), stable isotopes of hydrogen and oxygen in water, and inorganic carbon (δD, δ^{18}O, and $\delta^{13}C_{DIC}$). The findings indicate that the P_1s coal seam primarily contains HCO_3−Na type water, while the P_1t coal seam consists of Cl−Na and HCO_3−Na types of water. The disparity in water types between P_1s and P_1t can be attributed to interactions between water and rocks. The isotopic compositions of δD, δ^{18}O, and $\delta^{13}C_{DIC}$ suggest that the sampled coalbed waters originate from atmospheric precipitation, with subsequent microbial activity. It is suggested that TDS content along with bicarbonate concentration can serve as effective indicators for determining high productivity due to weaker hydraulic conditions and a more enclosed water environment in P_1t coal seams; threshold values being >1000 mg/L for TDS and >10 mequiv/L for bicarbonate concentration. Additionally, microbial activity is found to be more widespread in P_1t compared to P_1s. Principal component analysis reveals a significantly higher contribution of conventional ions toward TDS content observed within the P_1t coal seam compared to that of P_1s coal seam, accompanied by alterations in pH control parameters. The water produced from the P_1s coalbed is primarily controlled by evaporite and silicate weathering/dissolution coupled with substantial cation exchange. Conversely, the water in the P_1t coalbed is mainly influenced by silicate weathering/dissolution as well as evaporative concentration, with a limited occurrence of cation exchange. Moreover, there are distinct disparities in ion sources between P_1s and P_1t. These research findings provide a scientific foundation for assessing the development potential of CBM and optimizing extraction systems within similar CBM areas.

1. INTRODUCTION

The coalbed methane (CBM), recognized as an environmentally friendly and clean unconventional natural gas resource,[1−4] has been extensively exploited in major coal-producing regions, including China, the United States, Canada, and Australia.[5−8] The emergence of two CBM industrial zones in the southern part of the Qinshui Basin and the eastern part of the Ordos Basin is a notable indication that China has entered an initial stage of large-scale CBM development.[8] The process of CBM development typically leads to the generation of significant volumes of water.[9,10] The chemical composition of coalbed water can serve as a valuable indicator, reflecting the generation pathway and

Received: October 28, 2023
Revised: December 28, 2023
Accepted: December 29, 2023
Published: January 17, 2024

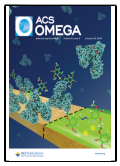

https://doi.org/10.1021/acsomega.3c08525
ACS Omega 2024, 9, 4905−4919

aiding in the production prediction of CBM, due to its active involvement in various processes associated with CBM generation and extraction.[10−13] The hydrogeochemical characteristics of coalbed water can thus be regarded as fundamental attributes in the exploration and development of CBM.

Previous research has indicated a global uniformity in the hydrochemistry of coalbed groundwater, characterized by the absence of sulfates, low levels of calcium and magnesium, and elevated concentrations of sodium, bicarbonate, and chloride.[13−20] The processes involved in this include salt dissolution, salt precipitation, pyrite oxidation, ion exchange, sulfate reduction, and methane generation.[13,17,18,21] The pH can influence these processes; for instance, an increase in silicate weathering of minerals such as albite can occur at a pH level above 8 due to the availability of OH^- ions. TDS can indicate the degree of confinement in coalbed water: lower TDS suggests a relatively open hydrodynamic environment, while higher TDS indicates a relatively closed hydrodynamic environment.[20] The Global Meteoric Water Line (GMWL), proposed by Craig,[22] has been extensively utilized in hydrogeochemical research to determine the origin of groundwater and identify water−rock interactions using stable isotopes of hydrogen and oxygen,[23,24] which are pivotal in this field.[25−27] Furthermore, studies have indicated that the stable isotope distribution within deep groundwater is associated with groundwater flow patterns, thus serving as a reliable tracer for water circulation.[28] The previous analysis of trace elements in CBM well water samples has indicated that specific trace elements, such as lithium (Li), gallium (Ga), rubidium (Rb), strontium (Sr), and barium (Ba), can be utilized for identifying water sources and predicting production potentials of CBM wells.[29,30] Conversely, limited research has been conducted on the presence of inorganic carbon in CBM well waters, primarily focusing on $\delta^{13}C(CO_2)$ values resulting from carbonate dissolution or thermogenic release. These values typically range around 0‰, while $\delta^{13}C(CO_2)$ values originating from organic matter generally fall below −8‰. It has been suggested that the higher concentrations of HCO_3^- observed in waters produced from CBM wells are linked to increased content levels and production capacities due to migration toward higher positions, along with CO_2 dissolution derived from CBM referred to as the "gas−water fractionation" phenomenon.[2−4,31]

A comprehensive understanding of the geochemical characteristics and origin mechanisms of coalbed water is essential for investigating the enrichment mechanism of CBM and guiding its exploration. The Baode block, situated on the eastern margin of the Ordos Basin, represents a typical area for CBM development. However, there remains a lack of an effective comprehension regarding the geochemical characteristics of its produced water. Hence, this study collected water samples produced from P_1s and P_1t Formations. By analyzing parameters such as pH, total dissolved solids (TDS), conventional ions, stable isotopes of hydrogen and oxygen, dissolved inorganic carbon isotopes, and trace elements, we have elucidated the hydrochemical types, ion composition characteristics, and variations in water sources among produced coal seams in the area. Principal component analysis was utilized to establish correlations between various hydrochemical parameters and their primary factors. Additionally, it aimed to investigate the indicative significance of characteristic trace elements and disparities in microbial activity within diverse coalbed waters while identifying sources and disparities of ions in groundwater environments. Ultimately, this study revealed hydrogeochemical disparities and constraints within distinct coal seams in the region. The research findings have significant theoretical and practical implications for predicting CBM well production capacity and optimizing extraction systems within similar CBM blocks.

2. GEOLOGICAL SETTINGS

The Baode block is one of the most successful and largest-scale mid-to-low-rank CBM fields in China, with a proven geological CBM reserve of 34.35×10^9 m^3. It is located on the eastern margin of the Ordos basin in China (Figure 1a,b). The tectonic position of the Baode block is within the northern portion of the Jinxi fault-fold belt. The main structure of the Baode block is relatively simple, generally exhibiting a prominent monocline with a significant northwestward dip. The western part of the block has gently dipping strata with angles of 3 to 7°, while the eastern part has relatively steeper dips of 5 to 10°, with some small-scale faults present locally (Figure 1d).[32]

The coal-bearing formations in the area primarily consist of the Shanxi and Taiyuan Formations (Figure 1c). The Shanxi Formation is characterized by fluvial and deltaic facies, with coal-bearing deposits ranging from 30 to 116 m in thickness. The lithology mainly comprises gray-white sandstone, siltstone, gray sandy shale, carbonaceous shale, and coal seams, totaling 6 to 8. The Taiyuan Formation represents marine-continental transitional facies with coal-bearing deposits. The lithology is primarily composed of black-gray sandy shale, gray-white medium-coarse sandstone, fine sandstone, gray limestone, marlstone, and coal seams amounting to a total of 7. In combination with both formations mentioned above, there are a total of 13 to15 coal seams present within them having an overall thickness ranging from 8 to 32 m. The main target coal seams for CBM exploration and development in the Baode block are the P_1s (no. 4 + 5) and the P_1t (no. 8 + 9), with a vertical spacing of 50 to 90 m between the two coal sets. The no. 4 + 5 and the no. 8 + 9 coal seams are located in the lower and middle sections of the P_1s and the P_1t, respectively, and they are well-developed and stable throughout the block. The maximum reflectance of vitrinite in the coal seams is between 0.79% and 1.15%, indicating middle- and low-rank coal.[32]

3. MATERIALS AND METHODS

3.1. Samples Collection. To comprehensively elucidate the geochemical characteristics of coalbed water in the Baode block and gain insights into the in situ environmental conditions and evolution of coalbed water, representative water samples were collected from coal seams. A total of 20 samples of coalbed-produced water were obtained from the production well. Samples ID B1 to B10 were gathered from no. 4 + 5 coal seam of P_1s Formation, while B11 to B20 were sampled from No. 8 + 9 coal seam of P_1t Formation. The distribution of the sampling wells is shown in Figure 1d, and detailed information about all sampling wells is presented in Table 1. Notably, these samples were collected from wells with a production duration of 8 months, ensuring that hydrochemical measurements accurately reflect the original formation water characteristics while avoiding any potential influence from fracturing fluid.

During the collection of produced water samples, high-density polyethylene (HDPE) sampling bottles were used to collect filtered water samples. The samples were used for testing cations, anions, stable isotopes of hydrogen and oxygen, TDS, pH, $\delta^{13}C_{DIC}$, and trace elements. To exclude the interference of

https://doi.org/10.1021/acsomega.3c08525
ACS Omega 2024, 9, 4905−4919

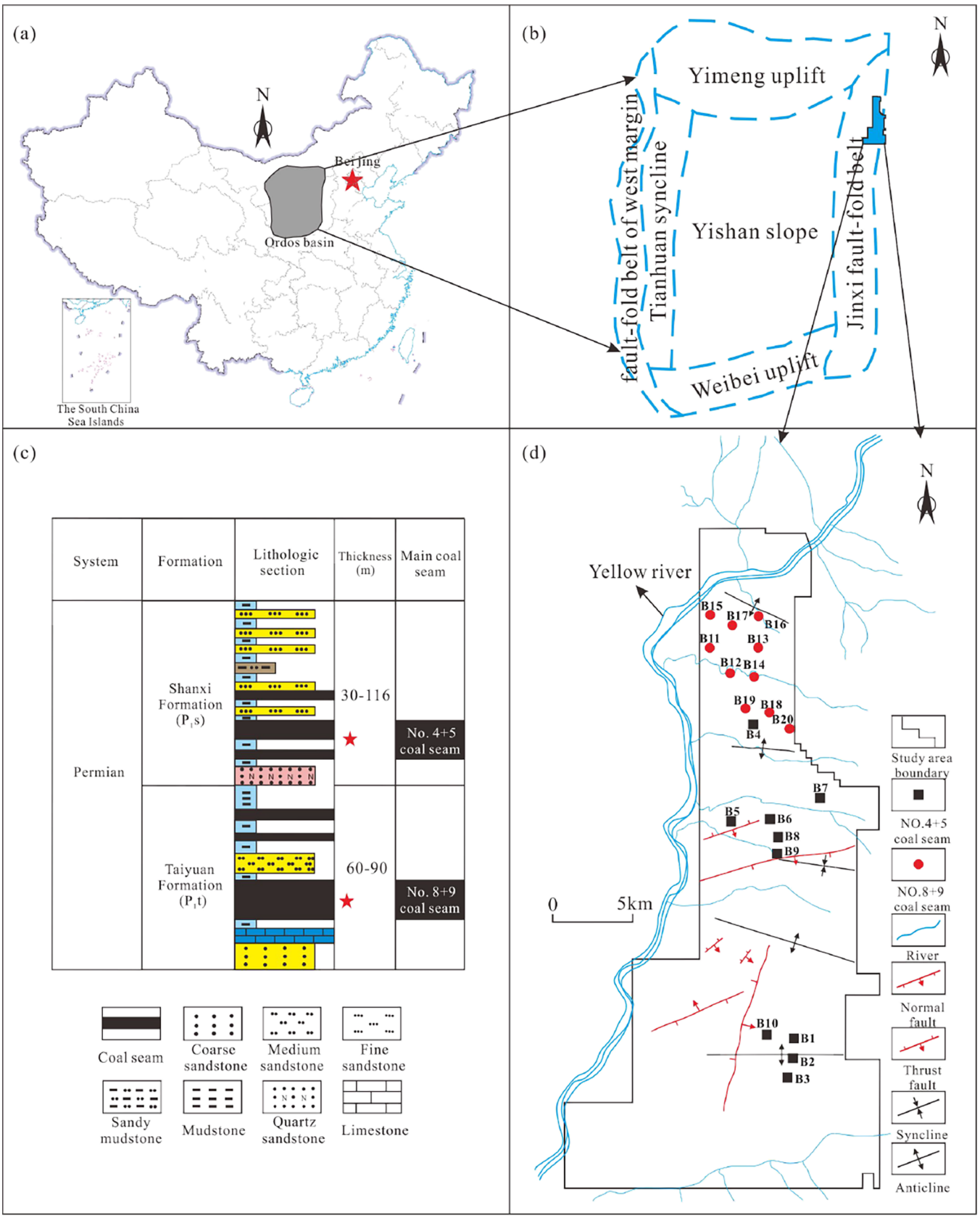

Figure 1. (a) Location map of Ordos basin, (b) structure outline of Ordos basin, (c) column diagram of coal seam,[32] and (d) structure outline and sampling locations of the Baode block.[32]

stagnant water in the wellbore and ensure the freshness of the collected samples, the production water valve was opened, and water was discharged for a period of time, followed by multiple rinses of the sampling bottles. To filter the samples, a peristaltic

https://doi.org/10.1021/acsomega.3c08525
ACS Omega 2024, 9, 4905−4919

Table 1. Basic Information about Coalbed Methane Sampling Wells[a]

sample ID	coal bed	depth (m)	gas rate (m^3/d)	gas production scale
B1	Shanxi Formation (no. 4 + 5)	969.0	450.92	low
B2		902.5	261.04	low
B3		992.0	324.00	low
B4		975.0	1213.27	high
B5		1140.0	781.24	middle
B6		843.0	514.08	middle
B7		636.5	224.64	low
B8		1035.0	280.00	low
B9		993.0	880.48	middle
B10		1047.0	781.24	middle
B11	Taiyuan Formation (no. 8 + 9)	1050.0	5634.63	high
B12		786.0	1642.02	high
B13		847.0	2192.08	high
B14		644.0	2645.29	high
B15		813.0	3383.63	high
B16		620.3	2253.07	high
B17		842.7	2174.35	high
B18		885.0	344.90	middle
B19		1079.5	3251.43	high
B20		781.0	2138.55	high

[a]The gas rate is classified as low if it is less than 500 m^3/d; it is classified as middle if it falls between 500 m^3/d and 1000 m^3/d; and it is classified as high if it exceeds 1000 m^3/d.

pump (Geotech) with Viton tubing and a PFA filter housing was used to push the water through a precombusted glass fiber membrane with 0.7 μm pores and then a polysulfone membrane with 0.2 μm pores. To preserve cations and trace elements, the samples were acidified with nitric acid to pH < 2 on-site. To ensure quality control of the test results, duplicates of some samples were collected.

3.2. Experimental Methods. Cation analysis was conducted on coalbed-produced water samples using an inductively coupled plasma-mass spectrometer (ICP-MS) instrument model: Vista MPX, USA). Anion analysis was carried out utilizing an ion chromatograph (instrument model: ICS-90, USA). Some key parameters included the use of an AG14-AS14 (4 × 250 mm) anion column, eluent composition of 8 mM Na_2CO_3/1 mM $NaHCO_3$, flow rate set at 1.2 mL/min, sample injection volume of 10 μL, detection by automatic regenerating anion micromembrane suppression conductivity detector, with a detection limit of 0.1 mg/L. Bicarbonate (HCO_3^-) and carbonate (CO_3^{2-}) ions were quantified through acid titration.

The hydrogen and oxygen isotope analyses were conducted using a liquid isotope analyzer (instrument model: 912−0026) based on the principles of laser spectroscopy and resonance attenuation. The precision of the instrument is demonstrated by a standard deviation of 0.6‰ for δD and 0.1‰ for δ^{18}O. The DIC isotope analysis was conducted using a gas isotope mass spectrometer (instrument model: MAT252), which has specifications including a resolution of 200, a mass range of 1−150 A, and precision values ≤0.01‰ for δ^{13}C.

The trace element analysis was conducted using an inductively coupled plasma−mass spectrometer (ICP-MS) (instrument model: NexION 300 X, USA). The pH analysis was performed by utilizing a pH meter (instrument model: PP-50-p11), and TDS analysis was carried out employing a conductivity meter (instrument DDSJ-308A). The test results can be found in Tables 2−4.

4. RESULTS AND ANALYSIS

4.1. Conventional Ion Characteristics of Coalbed-Produced Water. Table 2 shows that both the P_1s and P_1t coalbed produced waters exhibit weak alkalinity, with average

Table 2. Geochemical Parameters of Coalbed-Produced Water in Baode Block

	concentration of conventional ion (ppm)								
sample ID	Na^+	K^+	Ca^{2+}	Mg^{2+}	Cl^-	SO_4^{2-}	HCO_3^-	pH	TDS (ppm)
B1	309.43	36.77	14.52	8.67	158.14	0.12	727.61	7.42	891.46
B2	196.22	59.88	49.41	25.33	170.42	0.10	590.54	7.08	796.53
B3	249.82	52.77	49.04	23.07	174.14	0.10	664.84	7.17	881.26
B4	468.70	123.45	115.91	76.01	1010.57	0.08	645.62	7.25	2117.53
B5	393.18	39.83	27.64	10.62	197.09	0.08	833.93	7.4	1085.41
B6	291.64	32.99	14.64	5.81	130.50	0.07	671.24	7.3	811.27
B7	174.10	60.2	38.41	27.27	203.98	0.05	488.06	6.82	748.04
B8	261.56	22.45	23.65	9.49	92.87	0.10	654.59	7.48	737.32
B9	387.51	58.27	30.38	8.64	301.78	0.10	746.82	7.31	1159.99
B10	261.82	56.93	40.55	25.14	182.78	0.05	725.05	7.29	929.81
average	299.40	54.35	40.41	22.00	262.23	0.90	674.83	7.25	1015.86
B11	1113.70	165.15	555.16	153.95	3288.91	0.10	848.02	6.93	5700.88
B12	217.12	63.24	146.6	52.12	430.33	23.09	728.89	6.86	1296.95
B13	280.10	78.14	137.93	30.84	362.31	0.10	970.99	6.96	1374.82
B14	325.03	74.38	146.91	38.32	674.64	0.10	760.91	6.98	1639.74
B15	1004.20	162.33	444.24	126.34	2433.93	0.06	981.25	6.84	4661.73
B16	564.87	114.49	205.14	55.18	1142.53	0.10	1100.38	7.17	2632.40
B17	312.41	95.57	188.15	44.65	470.69	0.10	865.96	7.06	1544.45
B18	208.21	40.73	70.57	27.84	218.74	0.09	662.28	7.03	897.32
B19	372.52	94.21	250.52	154.81	1096.89	0.33	725.05	7.46	2331.81
B20	238.80	43.56	86.95	23.95	256.20	0.08	837.77	7.4	1068.43
average	463.70	93.18	223.22	70.80	1037.52	2.42	848.15	7.07	2314.85

https://doi.org/10.1021/acsomega.3c08525
ACS Omega 2024, 9, 4905−4919

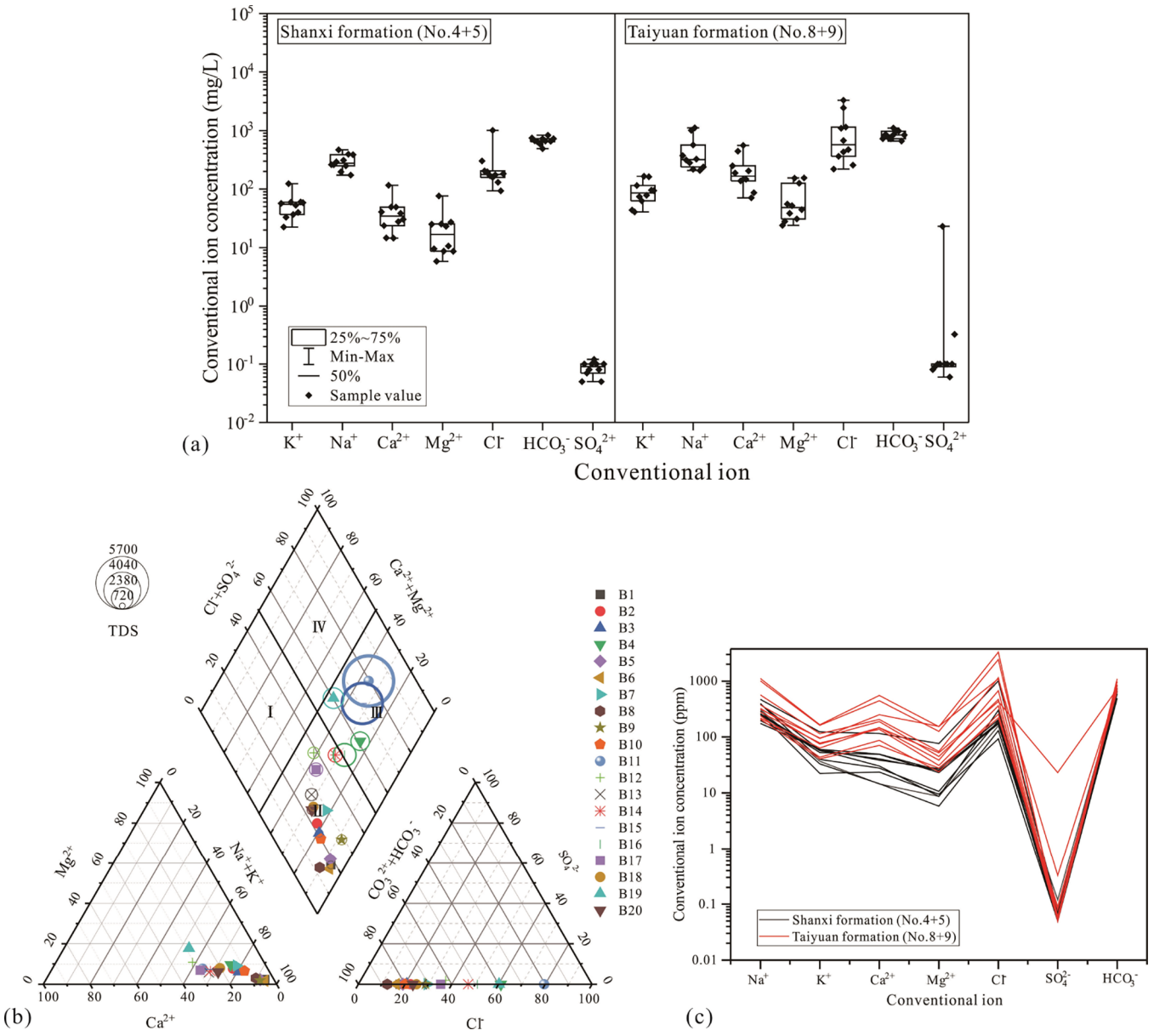

Figure 2. (a) Conventional ion box diagram, (b) Piper diagram, and (c) Schoeller diagram of coalbed-produced waters in Baode block (note: region I is river water or shallow groundwater, HCO_3−Ca type; region II is a deep groundwater, HCO_3−Na type; region III is SO_4−Na or Cl−Na type, usually seawater, salt water or hot water; region IV is a mixture of groundwater and salt water, SO_4−Ca or Cl−Ca type).

pH values of 7.25 and 7.07, respectively. There are distinct variations in the TDS and concentrations of certain common ions among different coalbed produced waters. In terms of TDS, the P_1t displays relatively higher TDS levels compared to the P_1s, with average values of 1015.86 and 2314.85 mg/L, respectively. As shown in Figure 2a, the coalbed produced waters from the P_1s and P_1t exhibit similar ion characteristics to CBM well produced waters from around the world, namely, higher concentrations of Na^+, Cl^-, and HCO_3^- and lower concentrations of Ca^{2+}, Mg^{2+}, and SO_4^{2-}.[17−20] In terms of differences in conventional ion concentrations (Figure 2a), the average concentration order of cations in the coalbed produced water of the P_1s is $Na^+ > K^+ > Ca^{2+} > Mg^{2+}$ and the anion concentration order is $HCO_3^- > Cl^-$, while in the coalbed produced water of the P_1t, the average concentration order of cations is $Na^+ > Ca^{2+} > K^+ > Mg^{2+}$ and the anion concentration order is $Cl^- > HCO_3^-$.

The identification of groundwater types is also a crucial indicator for elucidating the hydrochemical environment of groundwater. Overall, the coalbed produced water from P_1s can be predominantly characterized as HCO_3−Na type deep groundwater (except B4), while the coalbed produced water from P_1t primarily consists of Cl−Na and HCO_3−Na types, with a higher proportion of HCO_3−Na deep groundwater samples (Figure 2b). As evidenced by the Schoeller diagram (Figure 2c), in comparison to the coalbed produced water samples from P_1s, these from P_1t exhibit less consistency in terms of high-concentration ion sequence, transitioning from singularly HCO_3−Na type water to a coexistence of HCO_3−Na and Cl−Na types.

4.2. Hydrogen, Oxygen, and Carbon Isotopic Compositions of Samples. The δD and δ^{18}O values in the coalbed produced water of different coal seams reveals the following results (Table 3): the average δD values for the P_1s and the P_1t

https://doi.org/10.1021/acsomega.3c08525
ACS Omega 2024, 9, 4905−4919

Table 3. Hydrogen and Oxygen Isotopic and DIC Carbon Isotopic Compositions of Coalbed-Produced Water in Baode Block

sample ID	δD (‰)	δ^{18}O (‰)	$\delta^{13}C_{DIC}$ (‰)
B1	−122.20	−15.64	20.01
B2	−85.66	−11.55	23.71
B3	−90.31	−12.43	20.66
B4	−83.62	−11.59	2.95
B5	−88.67	−12.27	13.37
B6	−88.77	−12.27	2.89
B7	−93.52	−12.97	23.63
B8	−94.98	−13.20	−0.21
B9	−92.29	−13.29	6.15
B10	94.18	−13.23	14.75
average	−90.53	−12.54	12.79
B11	−83.06	−11.62	20.72
B12	−87.90	−12.43	14.04
B13	−86.67	−12.29	16.74
B14	−89.04	−12.38	14.25
B15	−85.88	−11.60	14.23
B16	−98.22	−13.72	18.00
B17	−90.62	−12.45	19.00
B18	−90.82	−12.24	10.13
B19	−90.91	−12.53	−0.61
B20	−90.00	−12.32	13.78
average	−88.41	−12.22	14.03

coalbed produced water are −90.53 and −88.41‰, while the average δ^{18}O values are −12.54 and −12.22‰, respectively. In comparison to the coalbed of P_1t, the δD and δ^{18}O of the P_1s coalbed produced water are more negative. The δD and δ^{18}O compositions of coalbed produced water can effectively reflect its sources.[14,23,24,27] The δD and δ^{18}O values of coalbed produced water samples from the P_1s and the P_1t in the Baode block fall near the GMWL and the China Meteoric Water Line (CMWL). The fitting equations are $\delta D = 8.9\delta^{18}O + 20.5$[22,33] and $\delta D = 6.5\delta^{18}O + 9.4$,[24] respectively. However, there are still some data points projected above (left side, D drift) and below (right side, ^{18}O drift) these lines (Figure 3). This suggests that

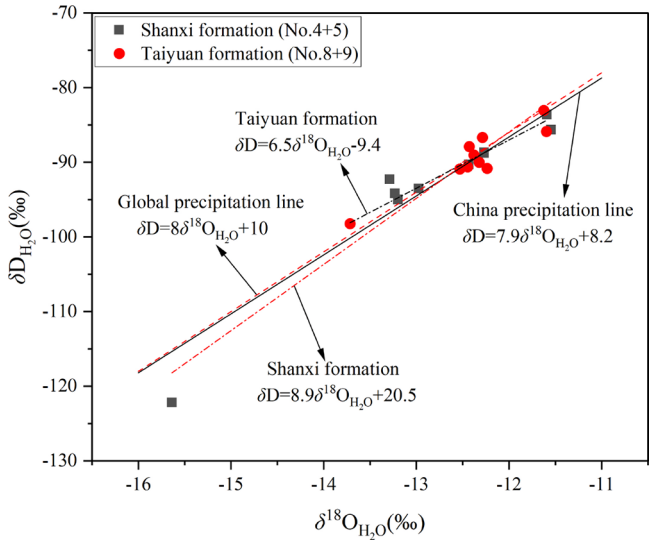

Figure 3. Relationship between $\delta D(H_2O)$ and $\delta^{18}O(H_2O)$ of coalbed-produced water in the Baode block.

the coalbed methane produced water in the study area primarily originates from atmospheric precipitation, but some samples exhibit slight ^{18}O and D isotopic variations, indicating that a range of geochemical processes such as evaporation, water−rock interactions, and methanogenesis may contribute to the generation and migration of coalbed methane produced water.[34−36]

The testing results of inorganic carbon isotope compositions in produced water are shown in Table 3. The range of $\delta^{13}C_{DIC}$ in the P_1s and the P_1t coalbed produced water is −0.21 to 23.71‰ and −0.61 to 20.72‰, respectively, with average values of 12.79 and 14.03‰.

4.3. Trace Elements Concentration in Coalbed-Produced Water. A total of 20 trace elements were tested in this study, including Li, V, Cr, Mn, Co, Ni, Cu, Zn, Ga, As, Rb, Sr, Zr, Nb, Mo, Sb, Ba, W, Hg, and Tl. Table 4 reveals the distribution of trace element concentrations in produced water from different coal seams (Figure 4a,b). It is observed that certain trace elements such as V, Cr, As, Zr, Nb, Sb, W, Hg, and Tl have extremely low levels, mostly below 1 ppb. These trace elements do not effectively reflect any characteristics. Therefore, we choose elements with stable distribution and relatively higher concentrations in the water samples for further analysis. Hence, we propose selecting Li, Mn, Co, Ni, Cu, Zn, Ga, Rb, Sr, Mo, and Ba, a total of 11 trace elements, for comparative analysis of their concentrations.

As depicted in Figure 4c, the overall mean concentrations of trace elements in the coalbed produced water of P_1t are larger compared to those in the P_1s. The element showing the largest difference between the two formations is Cu, while Ba, Sr, Mn, Li, Ga, and Rb exhibit varying concentrations but relatively high levels in both formations.

5. DISCUSSION

5.1. Indicative Significance of Trace Elements. The presence of trace elements in produced water reflects the origin of coal-bed-produced water and the gas production capacity of coalbeds. Previous studies have concluded that Li, Ga, Rb, Sr, and Ba can serve as characteristic trace elements for identifying the source of water and predicting CBM productivity.[29,30] These five elements are all reactive metals primarily found as inorganic constituents in coal, easily dissolving in water to form cations.[30] The concentrations of these five trace elements in the water produced from different coal seams in the Baode block are moderately high and exhibit significant variations, meeting the requirements for representativeness and distinguishability. Therefore, they are suitable as characteristic trace elements (Figure 4a).

Previous research on the geochemical characteristics of coalbed produced water in the Zhijin block in western Guizhou, found that the concentrations of these five trace elements in the produced water were positively correlated with their initial concentrations in coal.[31] It was confirmed that this correlation is the result of water-coal or water-rock interactions when groundwater flows through coal seams and their roof and floor strata, reflecting the intrinsic characteristics of coalbed water quality.[37] In this study, the average concentrations of trace elements in the produced water from P_1s and P_1t in the Baode block were analyzed for their correlation with the average concentrations of trace elements in the coal of the same area, showing a positive correlation (Figure 5a), supporting the above findings. It reveals that both the coalbed produced water from the P_1s and P_1t have undergone water−rock interactions with

https://doi.org/10.1021/acsomega.3c08525
ACS Omega 2024, 9, 4905−4919

Table 4. Results of Trace Element Concentration of Coalbed-Produced Water in Baode Block (unit, ppb)[a]

sample ID	Li	V	Cr	Mn	Co	Ni	Cu	Zn	Ga	As	Rb	Sr	Zr	Nb	Mo	Sb	Ba	W	Hg	Tl
B1	39.84	1.15	0.65	235.00	0.82	3.89	0.02	0.00	44.44	0.54	60.16	1204.95	1.92	9.67	18.29	7.82	998.17	6.51	1.30	0.30
B2	30.95	1.13	2.66	723.84	1.06	12.35	0.00	0.04	125.88	0.48	103.64	2711.81	0.93	4.67	2.45	2.11	2835.93	2.69	0.70	0.19
B3	65.47	1.27	0.56	605.80	1.06	5.03	0.00	0.00	89.69	0.01	97.37	2875.87	1.23	3.26	1.91	1.09	2022.62	2.05	0.55	0.15
B4	182.75	4.03	0.64	750.99	0.82	1.92	0.00	1.06	463.03	0.26	154.35	7221.78	1.04	2.47	6.05	0.83	10837.12	1.64	0.89	0.13
B5	146.47	0.90	2.63	198.18	0.41	17.29	0.81	34.71	128.05	0.15	68.23	3139.47	1.47	0.68	4.57	0.07	2976.58	0.48	0.12	0.05
B6	34.69	1.29	0.52	565.45	11.50	77.64	0.33	0.00	66.85	0.37	41.67	1034.62	1.64	0.56	56.79	0.85	1541.24	0.83	0.08	0.04
B7	385.54	1.18	0.25	1261.18	15.32	289.08	0.00	0.00	60.09	0.06	81.15	1886.11	0.25	0.53	20.49	0.09	1353.95	0.31	0.02	0.02
B8	53.01	0.75	0.52	126.70	0.87	9.42	0.00	0.00	80.50	0.00	38.72	1389.71	1.65	0.61	2.14	0.14	1842.21	0.73	0.08	0.03
B9	80.46	1.87	0.59	341.39	9.38	16.30	0.11	0.00	101.61	1.01	58.17	1710.67	1.13	0.51	9.15	0.29	2261.28	0.94	0.10	0.02
B10	122.16	0.93	0.43	97.96	0.33	51.64	0.08	0.00	139.54	0.00	97.58	3465.20	0.42	0.50	5.57	0.05	3172.41	0.65	0.04	0.02
average	114.13	1.45	0.95	490.65	4.16	48.46	0.14	3.58	129.97	0.29	80.11	2664.02	1.17	2.34	12.74	1.33	2984.15	1.68	0.39	0.10
B11	958.48	7.22	0.85	2182.51	6.31	9.80	17.87	44.26	2166.45	1.35	449.43	38080.66	0.38	0.43	0.70	0.01	52020.77	0.37	1.40	0.03
B12	143.78	1.39	0.70	1053.82	13.91	25.31	284.30	6.37	51.54	0.58	143.82	5145.84	0.91	0.35	2.73	0.08	1162.19	0.23	0.37	0.02
B13	362.48	2.29	1.24	760.29	5.16	8.43	10.86	14.27	442.27	0.44	154.21	4031.61	0.57	0.26	0.92	0.00	9011.51	0.14	0.04	0.02
B14	108.32	2.00	0.77	635.39	3.45	14.13	1.27	32.72	576.03	0.00	113.77	5308.94	0.73	0.34	0.45	0.01	12993.53	0.22	0.11	0.02
B15	919.33	7.60	0.88	967.49	7.51	20.57	1.27	13.84	1169.67	1.34	363.15	20696.33	0.42	0.34	4.44	0.09	27897.72	0.21	0.93	0.02
B16	189.04	2.13	0.89	1815.52	26.85	20.68	1.04	10.48	927.03	1.45	211.72	7245.03	0.44	0.28	4.62	0.02	20759.73	0.22	0.52	0.02
B17	224.89	1.57	0.64	270.61	1.79	5.62	18.88	40.18	534.12	0.31	209.38	4995.42	0.45	0.30	15.37	0.04	12136.19	0.27	0.24	0.02
B18	109.43	1.04	0.54	1030.09	0.92	7.09	0.76	74.21	251.78	0.00	79.13	3540.82	0.41	0.24	1.61	0.02	5699.23	0.18	0.01	0.01
B19	333.19	4.22	0.98	1182.09	0.66	1.53	4.86	21.14	379.13	3.70	167.21	12859.71	0.97	0.26	7.62	0.28	8897.08	0.12	0.13	0.02
B20	85.61	1.78	0.56	2334.39	81.76	19.72	455.09	8.90	290.63	0.52	69.19	3037.46	0.53	0.20	34.25	0.09	6693.84	0.20	0.06	0.02
average	343.46	3.12	0.80	1223.22	14.83	13.29	79.62	26.64	678.87	0.97	196.10	10494.18	0.58	0.30	7.27	0.06	15727.18	0.22	0.38	0.02

[a]The content is considered undetectable by the instrument when the value is 0.00.

https://doi.org/10.1021/acsomega.3c08525
ACS Omega 2024, 9, 4905−4919

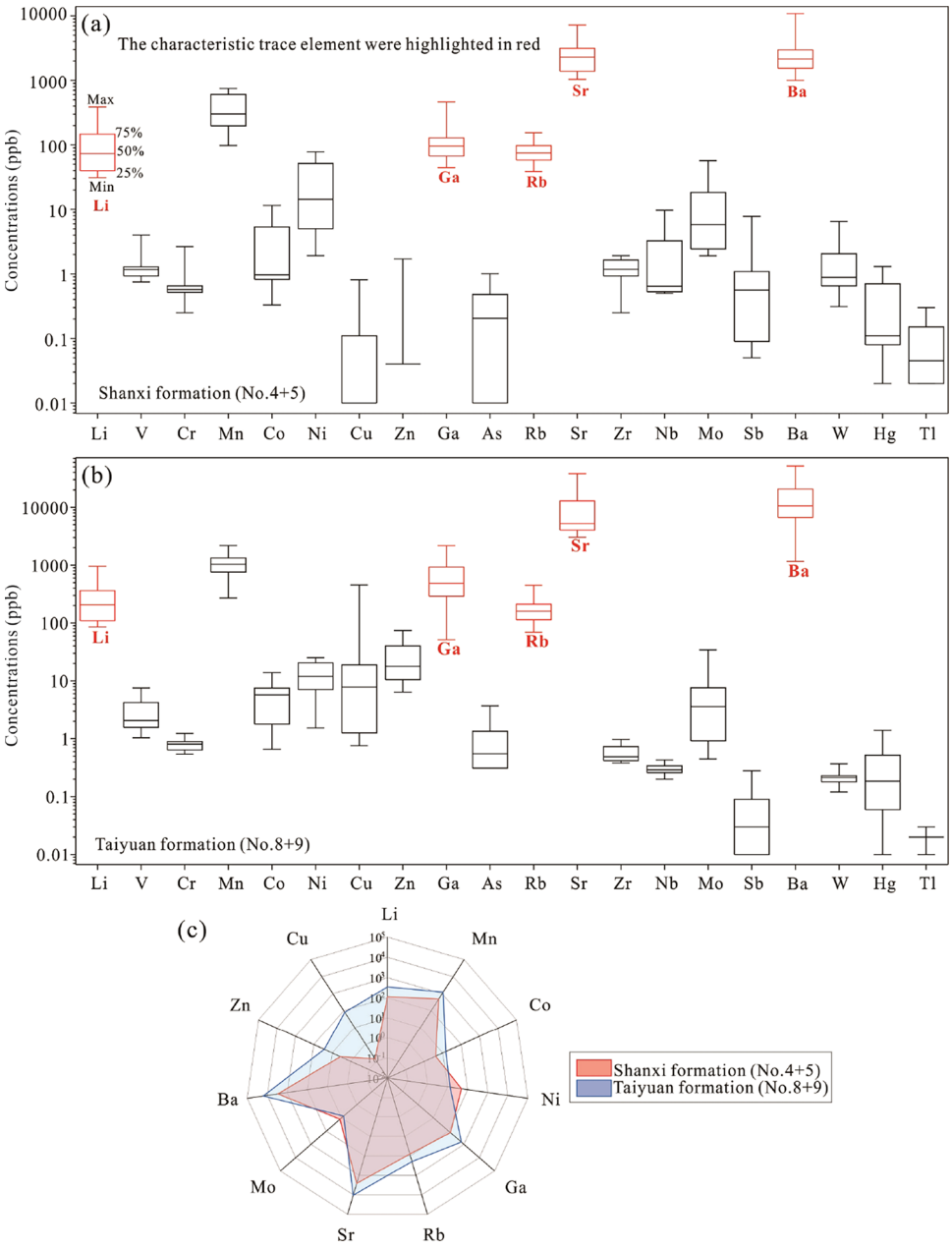

Figure 4. (a, b) Distribution of trace element concentrations and (c) comparison of trace element concentration in produced water of different coal seams.

the coalbed and adjacent rock layers. The average concentration of characteristic elements in the produced water from the P_1t is higher than that from the P_1s, indicating weaker hydrodynamics and a more confined water environment in the coalbed produced water from the P_1t (Figure 5b).

The TDS is a key parameter for evaluating the confinement of groundwater. During the subsurface flow of groundwater and its interaction with rocks, soluble mineral components in the rocks continuously dissolve, leading to an increase in TDS values along the direction of groundwater flow.[20] Additionally, characteristic trace elements such as Li and Rb undergo continuous changes within the dissolved mineral components (e.g., sodium feldspar).[4] Therefore, analyzing the relationship between these characteristic trace elements in groundwater can indirectly reflect the distribution characteristics of aquifer's groundwater flow field. In coalbed-produced water from P_1s and P_1t wells, both Li and Rb exhibit a positive correlation with both trace element concentrations and TDS levels (Figure 5c,d). Notably, higher concentrations in coalbed produced water from P_1t compared to that from P_1s. This reason is that sampling points for coalbed produced water in P_1s are predominantly located in the southern part of the block, where some areas have exposed faults. These areas are influenced by significant infiltration of atmospheric precipitation, surface water, and substantial influx from upper aquifers resulting in lower concentrations of characteristic trace elements as well as reduced TDS levels. Consequently, low TDS values, along with minimized HCO_3^- concentrations, are observed.

5.2. Microbial Activity of Water Produced from Various Coal Seams. Previous studies have indicated that the initial DIC in water primarily originates from CO_2, which readily dissolves in water and exists as H_2CO_3, HCO_3^-, and

https://doi.org/10.1021/acsomega.3c08525
ACS Omega 2024, 9, 4905−4919

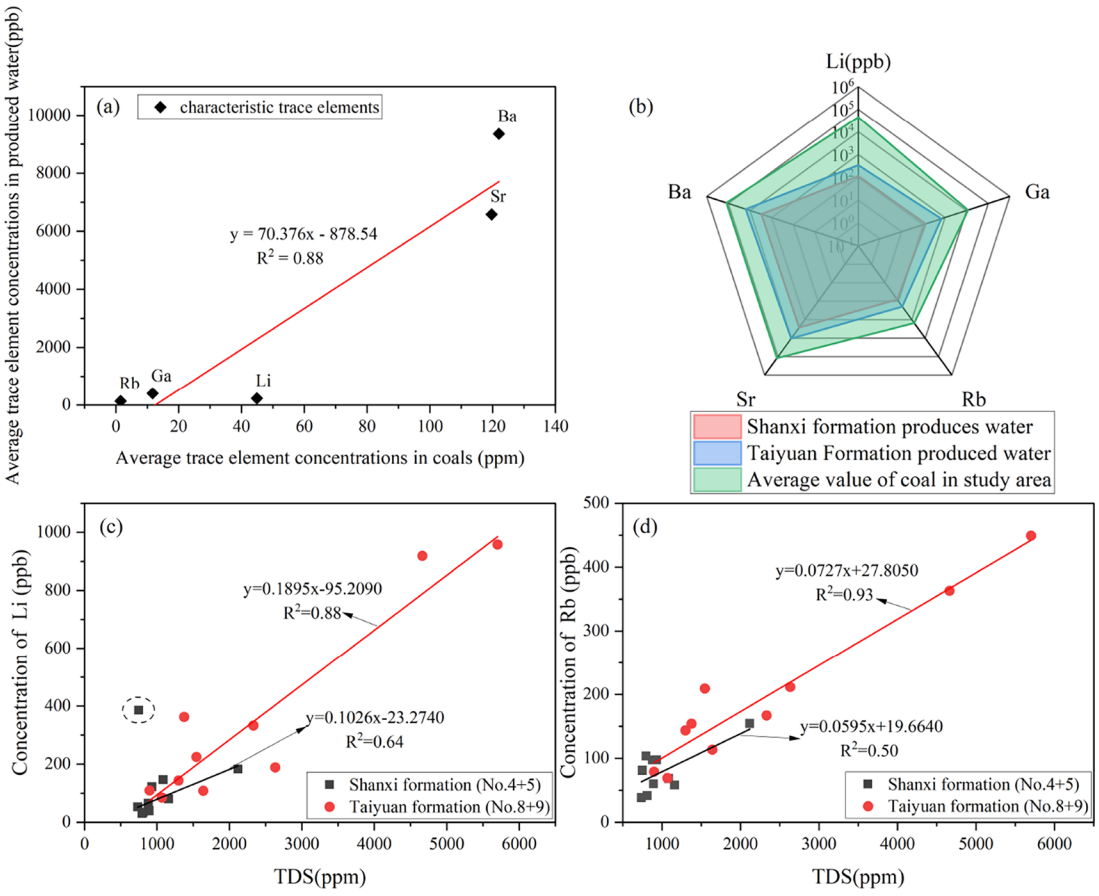

Figure 5. (a) Correlation between average concentrations of characteristic trace elements in coal and coalbed produced water in Baode block. Note: the data sourced from references 38 and 39 represents trace elements in coal; (b) spider diagram of characteristic trace element concentrations; (c) TDS vs Li and (d) TDS vs Rb relationships in Baode block coalbed-produced water samples.

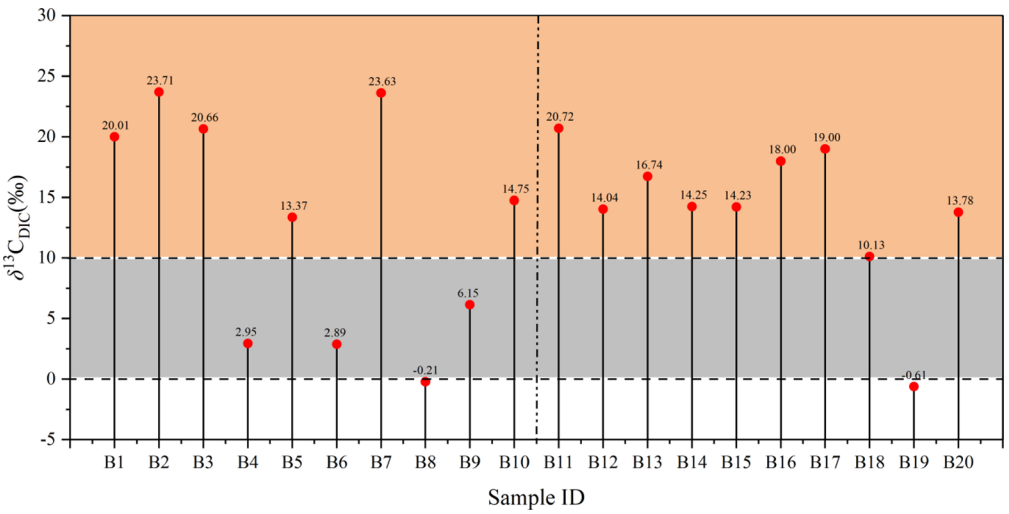

Figure 6. Distribution characteristics of $\delta^{13}C_{DIC}$ in coalbed-produced water.

CO_3^{2-}.[40] The $\delta^{13}C_{DIC}$ values of surface water and shallow groundwater generally range from −14 to −7‰, falling within an extremely low negative range.[14,15] In comparison, the $\delta^{13}C_{DIC}$ values in produced water from deep underground CBM wells are more enriched. This is generally represented by medium negative values ranging from −7 to 0‰.[14] However, microbial activity can result in a wider positive range of 10 to 30‰ for $\delta^{13}C_{DIC}$.[14] Among the various produced water samples collected from coal seams in the study area, more than half of them (15 samples) exhibit $\delta^{13}C_{DIC}$ values exceeding ten, including six samples from P_1s and nine samples from P_1t. This observation strongly suggests a significant presence of microbial activity within the coal seam in this area, with P_1t displaying a more extensive biological activity compared to P_1s (Figure 6).

Certain samples exhibit relatively low or even negative $\delta^{13}C_{DIC}$ values, which can be attributed to variations in the

https://doi.org/10.1021/acsomega.3c08525
ACS Omega 2024, 9, 4905−4919

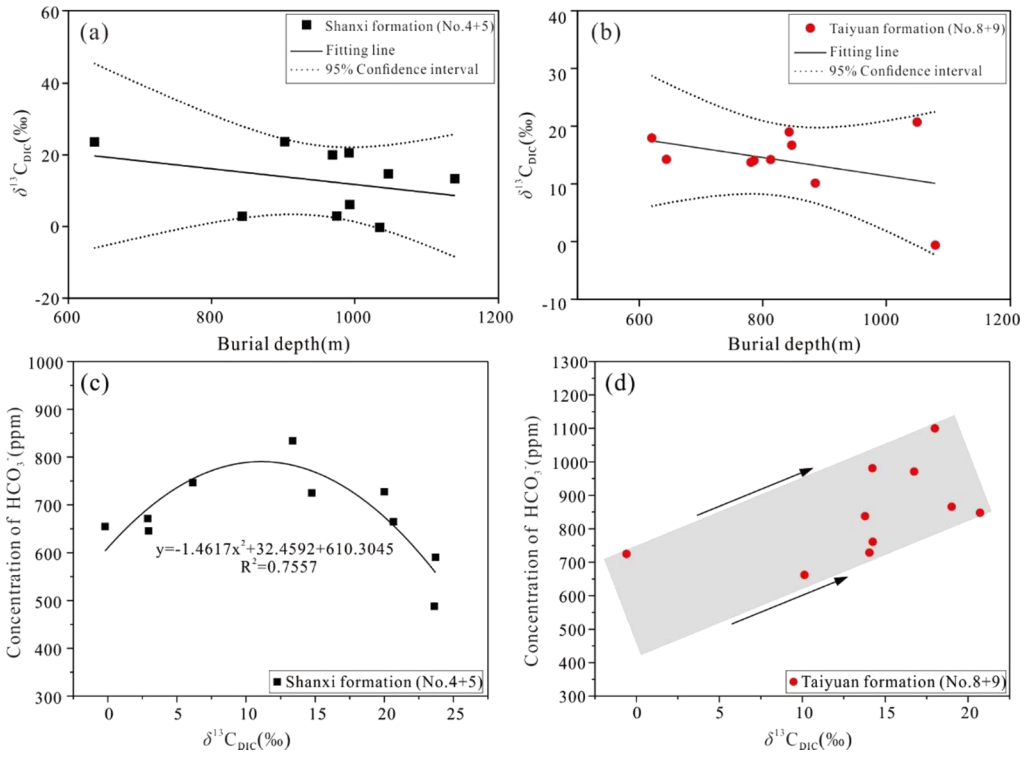

Figure 7. (a, b) $\delta^{13}C_{DIC}$ vs buried depth and (c, d) HCO_3^- of coalbed-produced water in the Baode block.

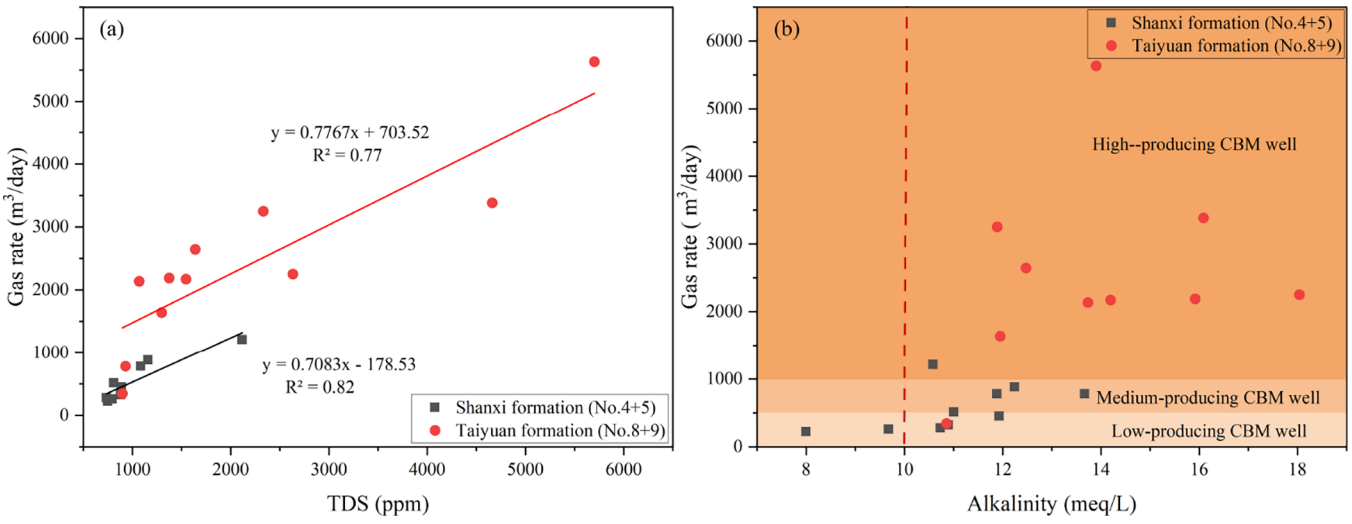

Figure 8. Correlations between (a) gas flow rate and TDS, and (b) gas flow rate and alkalinity.

dominant microbial metabolic pathways within coal seams resulting from changes in burial depth.[41] Consequently, these alterations have an effect on the $\delta^{13}C_{DIC}$ values observed in Figure 7a,b. The negative correlation between burial depth and $\delta^{13}C_{DIC}$ values further suggests the potential prevalence of CO_2 reduction pathways within microbial metabolisms occurring in coalbeds of the Baode block (as depicted by eqs 1 and 2).

$$CH_3COOH \rightarrow CH_4 + CO_2 \quad (1)$$

$$CO_2 + 4H_2 \rightarrow CH_4 + 2H_2O \quad (2)$$

The dissolved inorganic carbon isotope values and shallow groundwater generally exhibit a negative correlation with HCO_3^- concentration due to their primary source being ^{12}C. However, compared to soil carbonate minerals, carbonates in coal-bearing formations are more enriched in ^{13}C. Therefore, the relationship between dissolved inorganic carbon isotopes and bicarbonate may vary when they interact with groundwater. In the produced water from the P_1s coalbeds, there is an initial increase followed by a decrease in the relationship between the $\delta^{13}C_{DIC}$ and bicarbonate concentrations. The reason is that most sampling points are located in the southern part of the block where well-developed faults exist. After coal-water interactions and microbial processes occur, $\delta^{13}C_{DIC}$ values gradually increase in the produced water. However, exposed areas lead to the gradual mixing of surface water or shallow groundwater, intensifying microbial activity. Consequently, $\delta^{13}C_{DIC}$ values continue to rise while bicarbonate concentrations decrease (Figure 7c). In contrast, for the produced water from the P_1t

https://doi.org/10.1021/acsomega.3c08525
ACS Omega 2024, 9, 4905−4919

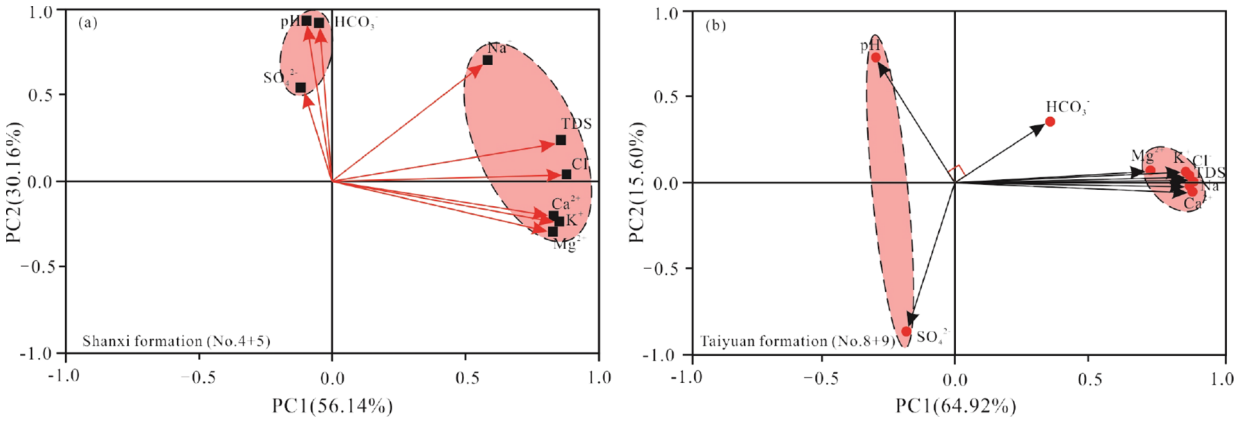

Figure 9. PCA analysis diagram of geochemical parameters of (a) No. 4 + 5 coal seam and (b) No. 8 + 9 coal seam produced water in Baode block.

coalbeds, there is a positive correlation between $\delta^{13}C_{DIC}$ and HCO_3^- concentrations because most sampling points are in the northern part of the block, where fewer faults exist, making it less susceptible to excessive mixing with surface water or shallow groundwater. Additionally, carbonate minerals from these coal seams, which are enriched in, undergo further interactions with water and microbial processes resulting in a positive correlation between HCO_3^- concentrations and $\delta^{13}C_{DIC}$ levels (Figure 7d).

5.3. Correlation between Various Geochemical Parameters of Coalbed-Produced Waters. The term "TDS" refers to the collective presence of ions, molecules, and compounds in groundwater, indicating the overall mineralization level. Higher mineralization suggests weaker hydraulic conditions that are conducive to CBM preservation and enrichment. A higher TDS value in associated water with the CBM indicates a greater proportion of pumping water originating from the coal seam itself rather than surrounding fractured sandstones or karst-fractured limestone aquifers. Increased discharge from the coal seam leads to reduced reservoir pressure, thereby enhancing CBM desorption and study area, both P_1s and P_1t exhibit a strong positive correlation between TDS levels in produced water and daily gas production highlighting the effectiveness of TDS as an indicator for assessing the production potential of CBM wells (Figure 8a).

Due to the limited impact of fracturing fluids on bicarbonate and its relatively minor variations, alkalinity can serve as a more precise indicator of CBM production compared to TDS.[10] In general, when the alkalinity concentration in produced water from CBM wells is less than 5 mequiv/L, it suggests the influence of fracturing fluids. The alkalinity concentrations of the produced water from P_1s and P_1t mostly exceed 10 mequiv/L, indicating minimal impact from fracturing fluids and productive performance. A level surpassing 10 mequiv/L typically corresponds to daily gas production greater than 500 m^3/d in CBM wells, classifying them as medium to high producers. Notably, most of the CBM wells in P_1t fall into the high production category (>1000 m^3/d) (Figure 8b). Therefore, for the Baode block's hydrologically more confined P_1t coal seams, bicarbonate concentration in produced water can effectively indicate the production of CBM wells.

Analyzing the correlation between geochemical parameters of produced waters is a convenient and effective method for studying the geochemical characteristics of coalbed produced water.[42,43] Principal component analysis (PCA), as a multivariate dimensionality reduction analysis method, allows us to analyze the relationships between multiple variables quickly and effectively.[25] To clarify the differences in the variable relationships among geochemical parameters in the produced water from different coal seams in the Baode block, we conducted PCA using SPSS v.21 (IBM Corp., USA) for the conventional ions, pH, and TDS of the P_1s and the P_1t coalbed produced water. The results are listed in Figure 9.

In the coal-bed-produced water of the P_1s, there is a clear positive correlation between HCO_3^- and pH. This suggests that HCO_3^- may further hydrolyze to generate OH^-, resulting in weak alkalinity in the produced water. It indicates that HCO_3^- plays an important role in the acidity and alkalinity of the coalbed produced water from the P_1s. TDS shows a positive correlation with Cl^-, Ca^{2+}, K^+, Mg^{2+}, and Na^+ ions, with Cl^- contributing the most to TDS (Figure 9a). However, in the produced water of the P_1t coal seam, there is no correlation observed between pH and HCO_3^-, but a negative correlation exists between the pH and SO_4^{2-}. TDS shows a significant positive correlation with Na^+, K^+, Ca^{2+}, Mg^{2+} and Cl^- ions, with Na^+ and Cl^- contributing the most to TDS (Figure 9b). The contribution of ions to TDS in the produced water from the P_1t coal seam is significantly greater than that from the P_1s coal seam, resulting in alterations to the pH control parameters. This can be attributed to weaker underground fluid dynamics and a more closed environment in the P_1t coal seam. Accumulation and retention of ions are more likely after precipitation, leading to higher contributions to TDS. Additionally, in this place, anaerobic microorganisms exhibit increased activity which strengthens devulcanization metabolic processes and leads to accumulation of intermediate products from anaerobic degradation - organic small molecule acids.[44] These factors contribute to differences in pH control mechanisms between P_1s and P_1t produced water.

5.4. Mechanism of Water-Rock Interactions. Based on Gibbs' research, the chemical composition of surface water worldwide can be classified into three main controlling models: atmospheric precipitation type, rock weathering type, and evaporation-concentration type.[45] Subsequently, based on these models, Gibbs I (Gibbs I= $Cl^-/(Cl^- + HCO_3^-)$) and Gibbs II (Gibbs II= $Na^+/(Na^+ + Ca^{2+})$) in relation to TDS were proposed as graphical templates (referred to as the Gibbs distribution model) for effectively identifying the chemical mechanisms of groundwater.

The chemical composition of the produced water from the P_1s coal seams is primarily controlled by the "rock dominant" type, the P_1t coal seams is influenced by both the "rock dominant" type and "evaporation dominance" type, with a greater influence

https://doi.org/10.1021/acsomega.3c08525
ACS Omega 2024, 9, 4905−4919

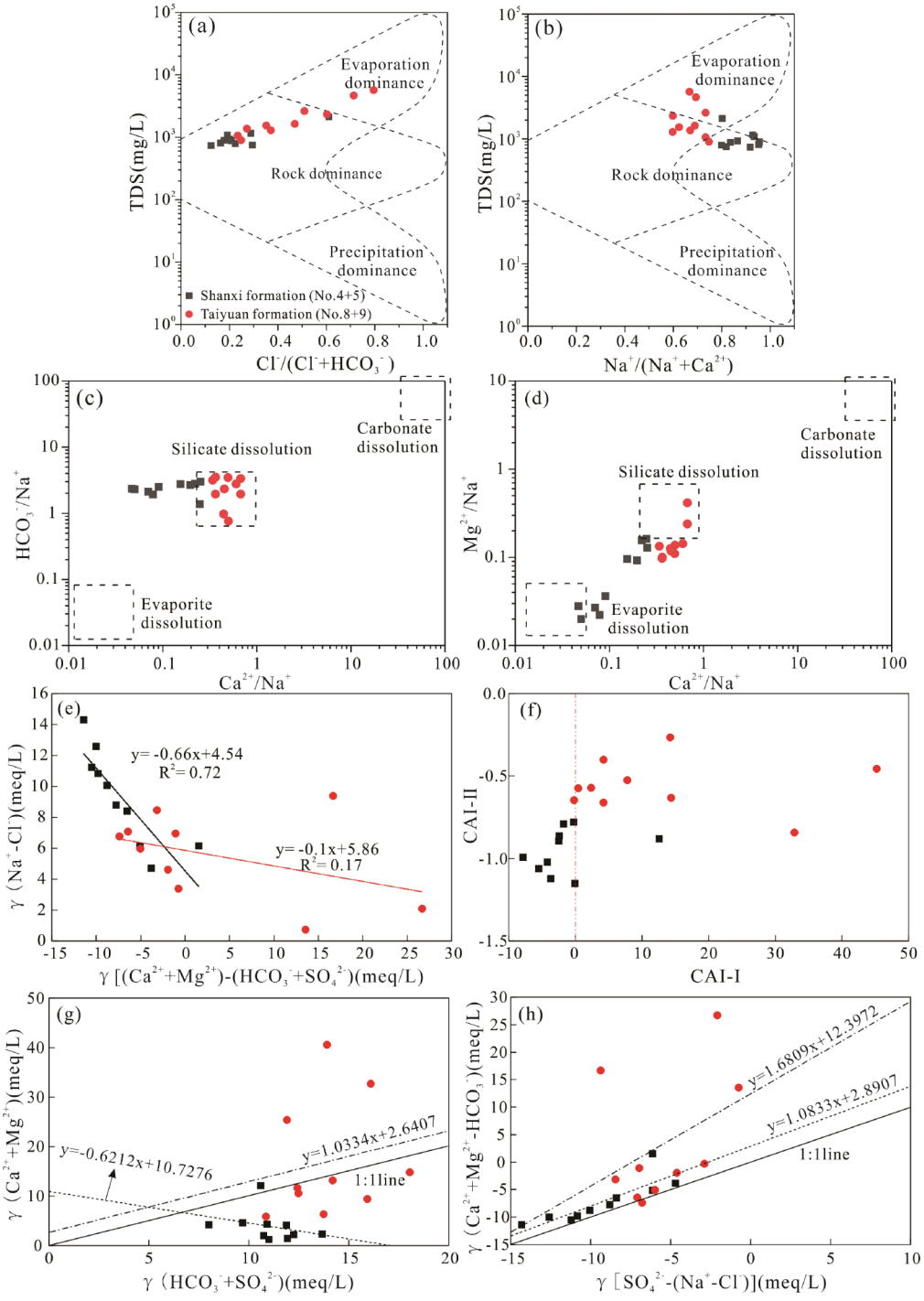

Figure 10. (a, b) Relationship between hydrochemical compositions of coal seam produced water in Baode block (Gibbs distribution model);[45] (c, d) Gaillardet diagram;[46] (e) molar ratio diagram of $[(Ca^{2+}+Mg^{2+}) - (HCO_3^{-}+SO_4^{2-})]$ vs $(Na^{+}-Cl^{-})$; (f) diagram of chlorine−alkaline index relationship; (g) molar ratio diagram of $(HCO_3^{-} + SO_4^{2-})$ vs $(Ca^{2+} + Mg^{2+})$; (h) molar ratio diagram of $[SO_4^{2-} - (Na^{+}-Cl^{-})]$ vs $(Ca^{2+} + Mg^{2+}-HCO_3^{-})]$. Note: the ionic unit is meq/L.

from the "rock dominant" type (Figure 10a, Figure 10b). Most data points in Figure 10b, representing water samples produced from the P_1s coal seams, are located outside of the "boomerang" shape but still indicate good aggregation. This could be attributed to prolonged water-rock interactions in groundwater within the coal seams during stagnant flowing periods, resulting in an expanded range of control by the "rock dominant" type. The observed good aggregation of sample points may also be associated with cation exchange processes.

In addition to Gibbs diagrams, the Gaillardet diagram can also be utilized for identifying solute sources in groundwater.[46] Based on the test data (Table 1), the Gaillardet diagram was plotted (Figures 10c and 10d). It is evident that evaporite and silicate dissolution jointly control the groundwater chemical composition of the P_1s coal seam, while silicate dissolution primarily influences P_1t coal seams.

Based on the analysis results obtained from Gibbs diagrams and Gaillardet end element diagrams, the initial understanding

https://doi.org/10.1021/acsomega.3c08525
ACS Omega 2024, 9, 4905−4919

of the contribution of water-rock interactions to the chemical composition of produced water from different coal seams in the Baode block can be elucidated. Previous studies have indicated that certain ratio relationships, such as γ (Na^+-Cl^-) to γ [(Ca^{2+} + Mg^{2+}) − (HCO_3^- + SO_4^{2-})], chloride-alkalinity indices (CAI-I and CAI-II), γ (Ca^{2+} + Mg^{2+}) to γ (HCO_3^- + SO_4^{2-}), γ (Ca^{2+} + Mg^{2+}-HCO_3^-) to γ [SO_4^{2-} − (Na^+-Cl^-)] can further reflect the source of ions in the produced water.[10,13,16,25] The produced water samples from the P_1s coal seams exhibit a significant negative correlation between γ[(Ca^{2+} + Mg^{2+}) − (HCO_3^- + SO_4^{2-})] and γ(Na^+-Cl^-), with a ratio close to −1, indicating cation exchange in the produced water from the P_1s coal seams. Conversely, a minimal occurrence of cation exchange is observed in the produced water from the P_1t coal seams (Figure 10e). From Figure 10f, it can be observed that CAI-I and CAI-II values for the produced water samples from the P_1s coal seams are negative (except for B4), indicating a strong and high-intensity occurrence of cation exchange adsorption (reaction mechanism shown in eq 3).[25]

$$(Na^+)(\text{rock}) + (Ca^{2+} + Mg^{2+})(H_2O) \rightarrow (Ca^{2+} + Mg^{2+})(\text{rock}) + (Na^+)(H_2O) \quad (3)$$

The Ca^{2+} and Mg^{2+} in groundwater primarily originate from the dissolution of carbonate or silicate and evaporative salt rocks. Therefore, the ratio of γ (Ca^{2+} + Mg^{2+}) and γ (HCO_3^- + SO_4^{2-}) equivalent can be utilized to determine the primary source of Ca^{2+} and Mg^{2+}.[25] As depicted in Figure 10g, the ratio of γ (Ca^{2+} + Mg^{2+}) and γ (HCO_3^- + SO_4^{2-}) in the produced water from the P_1s coal seam is approximately 0.62, significantly lower than 1. The primary hydrochemical process occurring in groundwater involves the dissolution of silicoaluminate minerals with Ca^{2+} and Mg^{2+} mainly originating from silicate and evaporite dissolution. On the other hand, for P_1t, this ratio generally aligns closely with a ratio of 1:1 (i.e., 1.03), suggesting that Ca^{2+} and Mg^{2+} predominantly arise from silicate dissolution. This is consistent with the results above (Figure 10c,d). The sources of SO_4^{2-} in groundwater mainly include sulfide oxidation and gypsum dissolution, among others. The origin of SO_4^{2-} can be determined by the ratio of γ (Ca^{2+} + Mg^{2+} − HCO_3^-) and γ [SO_4^{2-} − (Na^+-Cl^-)].[25] In general, the ratio of γ (Ca^{2+} + Mg^{2+} − HCO_3^-) and γ [SO_4^{2-} − (Na^+-Cl^-)] falls close to the 1:1 line at around 1.08 for produced water samples obtained from P_1s coal seam, indicating that SO_4^{2-} originates from gypsum and glauber's salt dissolution; however, for P_1t, it reaches approximately 1.68, which is considerably higher than 1, implying other influences on its source (Figure 10h).

6. CONCLUSIONS

Based on the testing and analysis of geochemical indicators such as cations, anions, stable isotopes of hydrogen and oxygen, total dissolved solids (TDS), pH, dissolved inorganic carbon isotopes ($\delta^{13}C_{DIC}$), and trace elements in the produced water from the P_1s and the P_1t coal seams in the Baode block, the following conclusions can be drawn.

(1) The hydrochemical compositions in the Baode block are characterized by relatively high concentrations of Na^+, Cl^-, and HCO_3^- while exhibiting low concentrations of Ca^{2+}, Mg^{2+}, and SO_4^{2-}. These characteristics are similar to coalbed-produced water worldwide. The water produced from P_1s coal seams is primarily classified as HCO_3−Na type, while that from P_1t coal seams is a combination of Cl−Na and HCO_3−Na types.

(2) The presence of characteristic trace elements (such as Li, Ga, Rb, Sr, and Ba) in the production water indicates a strong interaction between water and coal in this area, suggesting that P_1t has weaker hydrodynamics compared to P_1s with a more confined water environment. Moreover, $\delta^{13}C_{DIC}$ reveals widespread microbial activity within P_1t. Therefore, there exists a strong positive correlation between TDS levels and daily gas production, as well as a significant association between high bicarbonate concentration and CBM production. This suggests that the distribution patterns of TDS and bicarbonate concentration can effectively serve as indicators for identifying areas with high gas production within enclosed hydrogeological environments. It is recommended to set threshold values for TDS at levels exceeding 1000 mg/L, while bicarbonate concentration should exceed 10 mequiv/L.

(3) The principal component analysis reveals a significantly higher contribution of conventional ions to the TDS in the produced water from the P_1t coal seam compared to that from the P_1s coal seam, accompanied by changes in pH control parameters. The chemical composition of the produced water from the P_1s coal seams is primarily governed by weathering and dissolution of evaporite and cation exchange, while for the P_1t coal seams, it is mainly influenced by weathering and dissolution of silicate rocks and evaporation concentration with minimal occurrence of cation exchange.

AUTHOR INFORMATION

Corresponding Author

Yuan Bao − *College of Geology and Environment, Xi'an University of Science and Technology, Xi'an 710054, China*; orcid.org/0000-0001-6848-7431; Email: y.bao@foxmail.com

Authors

Yonghui Hao − *College of Geology and Environment, Xi'an University of Science and Technology, Xi'an 710054, China*

Zhidong Guo − *Institute of Engineering and Technology, PetroChina Coalbed Methane Company Limited, Xi'an 710082, China*

Yiliang Hu − *College of Geology and Environment, Xi'an University of Science and Technology, Xi'an 710054, China*

Jiajun Li − *College of Geology and Environment, Xi'an University of Science and Technology, Xi'an 710054, China*

Jiahao Meng − *College of Geology and Environment, Xi'an University of Science and Technology, Xi'an 710054, China*

Fei Wang − *College of Geology Engineering and Geomatics, Chang'an University, Xi'an, Shaanxi 710054, China*

Complete contact information is available at: https://pubs.acs.org/10.1021/acsomega.3c08525

Notes

The authors declare no competing financial interest.

ACKNOWLEDGMENTS

This work was supported by the National Natural Science Foundation of China (grant numbers: 42172200; 41972183)

and the Natural Science Basis Research Plan in Shaanxi Province of China (2022JM-147).

REFERENCES

(1) Bao, Y.; Wang, W.; Ma, D.; Shi, Q.; Ali, A.; Lv, D.; Zhang, C. Gas origin and constraint of $\delta^{13}C(CH_4)$ distribution in the Dafosi mine field in the southern margin of the Ordos Basin, China. *Energy Fuels* **2020**, *34* (11), 14065−14073.
(2) Bao, Y.; Ju, Y.; Yin, Z.; Xiong, J.; Wang, G.; Qi, Y. Influence of reservoir properties on the methane adsorption capacity and fractal features of coal and shale in the upper Permian coal measures of the South Sichuan coalfield, China. *Energy Explor. Exploit.* **2020**, *38* (1), 57−78.
(3) Yang, Z.; Qin, Y.; Qin, Z.; Yi, T.; Li, C.; Zhang, Z. Characteristics of dissolved inorganic carbon in produced water from coalbed methane wells and its geological significance. *Pet. Explor.* **2020**, *47* (5), 1074−1083.
(4) Yang, Z.; Wu, C.; Zhu, J.; Li, Y.; Qin, Z. Research progess on produced water geochemical from CBM wells in China. *Coal Sci. Technol.* **2019**, *47* (01), 110−117.
(5) Bao, Y.; Ju, Y.; Huang, H.; Yun, J.; Guo, C. Potential and constraints of biogenic methane generation from coals and mudstones from Huaibei coalfield, eastern China. *Energy Fuels* **2019**, *33* (1), 287−295.
(6) Li, Y.; Yang, J.; Pan, Z.; Meng, S.; Wang, K.; Niu, X. Unconventional natural gas accumulations in stacked deposits: a discussion of upper paleozoic coal-bearing strata in the east margin of the ordos basin. *China. Acta Geol Sin-Engl* **2019**, *93* (1), 111−129.
(7) Bao, Y.; Li, Z.; Meng, J.; Chen, X.; Liu, X. Reformation of coal reservoirs by microorganisms and its significance in CBM exploitation. *Fuel* **2024**, *360*, No. 130642.
(8) Qin, Y.; Moore, T. A.; Shen, J.; Yang, Z.; Shen, Y.; Wang, G. Resources and geology of coalbed methane in China: a review. *Int. Geol. Rev.* **2018**, *60* (5−6), 777−812.
(9) Kaiser, W.; Hamilton, D.; Scott, A.; Tyler, R.; Finley, R. Geological and hydrological controls on the producibility of coalbed methane. *J. Geol. Soc.* **1994**, *151* (3), 417−420.
(10) Zhang, S.; Tang, S.; Li, Z.; Pan, Z.; Shi, W. Study of hydrochemical characteristics of CBM co-produced water of the Shizhuangnan Block in the southern Qinshui Basin, China, on its implication of CBM development. *Int. J. Coal Geol.* **2016**, *159*, 169−182.
(11) Singh, A. P.; Gupta, S. K.; Mendhe, V. A.; Mishra, S. Variations in hydro-chemical properties and source insights of coalbed methane produced water of Raniganj Coalfield, Jharkhand, India. *J. Nat. Gas Sci. Eng.* **2018**, *51*, 233−250.
(12) Bao, Y.; Hu, Y.; Huang, H.; Meng, J.; Zheng, R. Evidence of coal biodegradation from coalbed-produced water − A case study of Dafosi gas field, Ordos Basin, China. *ACS Omega* **2023**, *44* (8), 41885−41896.
(13) Van Voast, W. A. Geochemical signature of formation waters associated with coalbed methane. *AAPG Bull.* **2003**, *87* (4), 667−676.
(14) Golding, S. D.; Boreham, C. J.; Esterle, J. S. Stable isotope geochemistry of coal bed and shale gas and related production waters: A review. *Int. J. Coal Geol.* **2013**, *120*, 24−40.
(15) Kinnon, E.; Golding, S.; Boreham, C.; Baublys, K.; Esterle, J. Stable isotope and water quality analysis of coal bed methane production waters and gases from the Bowen Basin, Australia. *Int. J. Coal Geol.* **2010**, *82* (3−4), 219−231.
(16) Owen, D. D.; Raiber, M.; Cox, M. E. Relationships between major ions in coal seam gas groundwaters: Examples from the Surat and Clarence-Moreton basins. *Int. J. Coal Geol.* **2015**, *137*, 77−91.
(17) Taulis, M.; Milke, M. Coal seam gas water from Maramarua, New Zealand: characterisation and comparison to United States analogues. *J. Hydrol.* **2007**, 1−17.
(18) Taulis, M.; Milke, M. Chemical variability of groundwater samples collected from a coal seam gas exploration well, Maramarua, New Zealand. *Water Res.* **2013**, *47* (3), 1021−1034.
(19) Wang, B.; Sun, F.; Tang, D.; Zhao, Y.; Song, Z.; Tao, Y. Hydrological control rule on coalbed methane enrichment and high yield in FZ Block of Qinshui Basin. *Fuel* **2015**, *140*, 568−577.
(20) Yao, Y.; Liu, D.; Yan, T. Geological and hydrogeological controls on the accumulation of coalbed methane in the Weibei field, southeastern Ordos Basin. *Int. J. Coal Geol.* **2014**, *121*, 148−159.
(21) Brinck, E. L.; Drever, J. I.; Frost, C. D. The geochemical evolution of water coproduced with coalbed natural gas in the Powder River Basin, Wyoming. *Environ. Geosci.* **2008**, *15* (4), 153−171.
(22) Craig, H. Isotopic variations in meteoric waters. *Science* **1961**, *133* (3465), 1702−1703.
(23) Chen, L.; Gui, H.; Yin, X. Monitoring of flow field based on stable isotope geochemical characteristics in deep groundwater. *Environ. Monit. Assess.* **2011**, *179*, 487−498.
(24) Zheng, S. H.; Hou, G.; Ni, B. Study on hydrogen and oxygen stable isotopes of meteoric water in China. *Chin. Sci. Bull.* **1983**, *13*, 801−806.
(25) Bao, Y.; An, C.; Wang, C.; Guo, C.; Wang, W.; Meng, Y. Hydrogeochemical characteristics and water−rock interactions of coalbed-produced water derived from the Dafosi biogenic gas field in the southern margin of Ordos basin, China. *Geofluids* **2021**, *2021*, No. 5972497.
(26) Bozau, E.; Licha, T.; Ließmann, W. Hydrogeochemical characteristics of mine water in the Harz Mountains, Germany. *Geochemistry* **2017**, *77* (4), 614−624.
(27) Hao, C.; Huang, Y.; He, P.; Sun, W. Isotope drift characteristics in Ordovician limestone karst water caused by coal mining in northern China. *Mine Water Environ.* **2019**, *38* (3), 507−516.
(28) Wang, S.; Tang, S.; Mo, Y.; Li, Z.; Zhang, S. The hydrogen and oxygen isotope characteristics of drainage water from Taiyuan coal reservoir. *J. China Coal Soc.* **2013**, *38* (3), 448−454.
(29) Qin, Y.; Zhang, Z.; Bai, J.; Liu, D.; Tian, Y. Source apportionment of produced-water and feasibility discrimination of commingling CBM production from wells in Southern Qinshui Basin. *J. China Coal Soc.* **2014**, *39* (9), 1892−1898.
(30) Yang, J. The periodic law of trace elements in coal—A case study of the 5# coal from the Weibei Coalfield. *Sci. China: Earth Sci.* **2011**, *54*, 1542−1550.
(31) Yang, Z.; Wu, C.; Zhang, Z.; Jin, J.; Zhao, L.; Li, Y. Geochemical significance of CBM produced water: A case study of developed test wells in Songhe block of Guizhou province. *J. China Univ. Min. Technol.* **2017**, *46*, 710−717.
(32) Chen, H.; Tian, W.; Chen, Z.; Zhang, Q.; Tao, S. Genesis of coalbed methane and its storage and seepage space in Baode Block, Eastern Ordos Basin. *Energies* **2022**, *15* (1), 81.
(33) Guo, Z.; Bao, Y.; Wang, Y.; Yuan, Y.; Li, Z.; Wang, Y.; Xia, L.; Liu, W.; Ma, J. Hydrogeochemical characteristics and water-rock interaction mechanism of coalbed-produced water in the Linfen mining area, eastern margin of Ordos Basin, China. *Front. Earth Sci.* **2023**, *10*, No. 1108520.
(34) Awaleh, M. O.; Baudron, P.; Soubaneh, Y. D.; Boschetti, T.; Hoch, F. B.; Egueh, N. M.; Mohamed, J.; Dabar, O. A.; Masse-Dufresne, J.; Gassani, J. Recharge, groundwater flow pattern and contamination processes in an arid volcanic area: Insights from isotopic and geochemical tracers (Bara aquifer system, Republic of Djibouti). *J. Geochem. Explor.* **2017**, *175*, 82−98.
(35) Talavera Mendoza, O.; Ruiz, J.; Díaz Villaseñor, E.; Ramírez Guzmán, A.; Cortés, A.; Salgado Souto, S. A.; Dótor Almazán, A.; Rivera Bustos, R. Water-rock-tailings interactions and sources of sulfur and metals in the subtropical mining region of Taxco, Guerrero (southern Mexico): A multi-isotopic approach. *Appl. Geochem.* **2016**, *66*, 73−81.
(36) Taheri, M.; Mahmudy Gharaie, M. H.; Mehrzad, J.; Afshari, R.; Datta, S. Hydrogeochemical and isotopic evaluation of arsenic contaminated waters in an argillic alteration zone. *J. Geochem. Explor.* **2017**, *175*, 1−10.
(37) Guo, C.; Qin, Y.; Xia, Y.; Ma, D.; Han, D.; Chen, Y.; Chen, W.; Jian, K.; Lu, L. Geochemical characteristics of water produced from CBM wells and implications for commingling CBM production: a case

https://doi.org/10.1021/acsomega.3c08525
ACS Omega 2024, 9, 4905−4919

study of the Bide-Santang Basin, western Guizhou, China. *J. Pet. Sci. Eng.* **2017**, *159*, 666−678.
(38) Dai, S. *Geological−geochemical behaviors and enrichment models of associated elements in coal*. China University of Mining & Technology Beijing, China, 2002.
(39) Yang, N.; Tang, S.; Zhang, S.; Xi, Z.; Li, J.; Yuan, Y.; Guo, Y. In seam variation of element-oxides and trace elements in coal from the eastern Ordos Basin, China. *Int. J. Coal Geol.* **2018**, *197*, 31−41.
(40) Chen, Y.; Qin, Y. Characterization and mechanism of exchange reaction through gas-water interface of gaseous inorganic CO_2. *J. China Coal Soc.* **2017**, *42* (07), 1811−1817.
(41) Woltemate, I.; Whiticar, M.; Schoell, M. Carbon and hydrogen isotopic composition of bacterial methane in a shallow freshwater lake. *Limnol. Oceanogr.* **1984**, *29* (5), 985−992.
(42) Helstrup, T.; Jørgensen, N. O.; Banoeng-Yakubo, B. Investigation of hydrochemical characteristics of groundwater from the Cretaceous-Eocene limestone aquifer in southern Ghana and southern Togo using hierarchical cluster analysis. *Hydrogeol. J.* **2007**, *15*, 977−989.
(43) Steinhorst, R. K.; Williams, R. E. Discrimination of groundwater sources using cluster analysis, MANOVA, canonical analysis and discriminant analysis. *Water Resour. Res.* **1985**, *21* (8), 1149−1156.
(44) Zhao, N.; Zhang, Y.; Zhao, X.; Yang, N.; Wang, Z.; Guo, Z.; Tong, J.; Zhang, Y.; Liu, Z. Hydrodynamic field driving effect and mathematical model construction of water quality formation and evolution in coal mine. *J. China Coal Soc.* **2023**, 1−15.
(45) Simpson, E. H. Measurement of diversity. *Nature* **1949**, *163* (4148), 688−688.
(46) Mukherjee, A.; Fryar, A. E. Deeper groundwater chemistry and geochemical modeling of the arsenic affected western Bengal basin, West Bengal, India. *Appl. Geochem.* **2008**, *23* (4), 863−894.

https://doi.org/10.1021/acsomega.3c08525
ACS Omega 2024, 9, 4905−4919